Inter- and Intraobserver Variability of an Anatomical Landmark-Based, Manual Segmentation Method by MRI for the Assessment of Myosteatosis and Sarcopenia in Subjects from the General Population

Running Title: Reproducibility of Myosteatosis and Sarcopenia by MRI

Lena S. Kiefer, MD[1], Jana Fabian[1], BS, Roberto Lorbeer, PhD[2], Jürgen Machann, PhD[3,4,5], Corinna Storz, MD[1], Mareen S. Kraus, MD[1], Elke Wintermeyer, MD[6], Christopher L. Schlett, MD MPH[7], Frank Roemer, MD[8], Susanne Rosplecz[9], MSc., Konstantin Nikolaou, MD[1], Annette Peters, PhD[9,10,11], Fabian Bamberg, MD MPH[1,9]

[1] Department of Diagnostic and Interventional Radiology, University of Tuebingen, Tuebingen, Germany
[2] Institute of Clinical Radiology, Ludwig-Maximilian-University Hospital, Munich, Germany
[3] Section of Experimental Radiology, Department of Diagnostic and Interventional Radiology, University of Tuebingen, Tuebingen, Germany
[4] Institute for Diabetes Research and Metabolic Diseases (IDM) of the Helmholtz Center Munich at the University of Tuebingen, Tuebingen, Germany
[5] German Center for Diabetes Research (DZD)
[6] BG Trauma Center, University of Tuebingen, Tuebingen, Germany
[7] Department of Radiology, Diagnostic and Interventional Radiology, University of Heidelberg, Heidelberg, Germany
[8] Department of Radiology, University of Erlangen-Nuremberg, Erlangen, Germany
[9] German Center for Cardiovascular Disease Research (DZHK e.V.), Munich, Germany
[10] Institute for Cardiovascular Prevention, Ludwig-Maximilian-University-Hospital, Munich, Germany
[11] Institute of Epidemiology II, Helmholtz Zentrum München, German Research Center for Environmental Health, Neuherberg, Germany

Type of manuscript: Full paper

Address for Correspondence:
Fabian Bamberg, MD MPH
Department of Diagnostic and Interventional Radiology
University of Tuebingen
Hoppe-Seyler-Straße 3
72076 Tuebingen
Germany
Phone: +49 7071 29 86676
Fax: +49 7071 29 5845
Email: fabian.bamberg@uni-tuebingen.de

Inter- and Intraobserver Variability of an Anatomical Landmark-Based, Manual Segmentation Method by MRI for the Assessment of Myosteatosis and Sarcopenia in Subjects from the General Population

<u>Running Title</u>: Reproducibility of Myosteatosis and Sarcopenia by MRI

ABSTRACT

Objectives: Changes in skeletal muscle composition, such as adipose content and mass, may exert unique metabolic and musculoskeletal risks; however, its reproducibility remains unknown. We determined the variability of the assessment of myosteatosis and sarcopenia by magnetic resonance imaging (MRI) in a sample from the general population.

Methods: We included a random sample from a prospective, community-based cohort study (KORA-FF4). Skeletal muscle adipose content was quantified as proton-density fat-fraction (PDFF) and mass as cross-sectional area (CSA) in multi-echo Dixon sequences (TR 8.90ms, six echo times, flip-angle 4°) by a standardized, anatomical landmark-based, manual skeletal muscle segmentation at level L3 vertebra by two independent observers. Reproducibility was assessed by intra-class correlation coefficients (ICC), scatter and Bland-Altman plots.

Results: In 50 included subjects (mean age 56.1±8.8years, 60.0% males, mean BMI 28.3±5.2) 2'400 measurements were obtained. Inter-observer agreement was excellent for all muscle compartments (PDFF: ICC0.99, CSA: ICC0.98) with only minor absolute and relative differences (-0.2±0.5%, 31±44.7mm^2; -2.6±6.4% and 2.7±3.9%, respectively). Intra-observer reproducibility was similarly excellent (PDFF: ICC1.0, 0.0±0.4%, 0.4%; CSA: ICC1.0, 5.5±25.3mm^2, 0.5%, absolute and relative differences, respectively). All agreement was independent of age, gender, BMI and body height (ICC0.96-1.0). In addition, PDFF-reproducibility was independent of CSA (ICC0.93-0.99).

Conclusions: Quantification of skeletal muscle adipose content and mass by MRI is highly reproducible and may therefore serve as a robust proxy for myosteatosis and sarcopenia in large cohort studies.

Advances in knowledge: An anatomical landmark-based, skeletal muscle segmentation provides high reproducibility and may therefore serve as a robust proxy for myosteatosis and sarcopenia.

INTRODUCTION

Skeletal muscle represents an essential organ system, determining the physical condition and serving locomotion, physical activity and mobility, but also playing a crucial role in the energy metabolism and hormone homeostasis of the organism.[1,2] It may therefore serve as an ideal target for health preservation and/or improvement.[3,4] In fact, changes in skeletal muscle composition, for example variation of intramuscular adipose content or alteration of skeletal muscle mass, are associated with various chronic disease conditions, such as diabetes mellitus (DM) or sarcopenia.[5–9] With more than 833 million people worldwide being affected by DM and its precursor stage prediabetes[10] and an estimated prevalence of sarcopenia up to 50% for patients aged 80 years and older[11], the socioeconomic impact of both entities is substantial but interactions are still not well understood.

Since skeletal muscle is a major target organ of insulin, recent data suggest that patients with DM are at high risk for skeletal muscle depletion.[9] Specifically, type 2 diabetes mellitus (T2DM) is associated with an increased prevalence of sarcopenia, impaired mobility and physical disability while myosteatosis has been identified as an effect modifier in DM.[9,12–17] Despite these early data, it remains unclear to what extent ectopic lipid depots in skeletal muscle contribute to the development and progression of insulin resistance and, conversely, how T2DM per se is associated with the successive depletion of skeletal muscle mass, strength and function. Hence, large cohort studies are needed to gain profound insights into the pathophysiological relevance of myosteatosis and sarcopenia and its correlation with DM as potential diagnostic or prognostic factors.

For this purpose, magnetic resonance imaging (MRI) seems to be particularly suited to analyze skeletal muscle composition, considering its non-ionizing and non-invasive nature as well as high soft tissue contrast.[18–21] The feasibility of this approach depends on a robust and reliable method for the quantification of skeletal muscle biomarkers, such as skeletal muscle adipose content and mass. However, the reproducibility of these biomarkers by MRI in a cohort setting remains unknown.

We therefore determined the reproducibility of the MR-based quantification of skeletal muscle adipose content and mass using an anatomical landmark-based, manual segmentation approach in a sample from a general population. Our hypothesis was that such an approach will be robust and highly reproducible and may therefore serve as a reference for future studies.

MATERIALS AND METHODS

Study design and population

Subjects were derived from the KORA-FF4 study (2013-2014, n=1851), a 14-year follow-up study of the population-based Cooperative Health Research in the Region of Augsburg (KORA) survey S4 (1999-2001, n=4261). The design of the KORA studies has been described in detail previously.[22,23] The study was approved by the local institutional review board of the Ludwig-Maximilian-University Munich, written informed consent was obtained from all participants. Subjects underwent a whole-body MRI according to the following inclusion (willingness to undergo MRI examination, signed informed consent form) and exclusion criteria (age > 72years, validated/self-reported history of stroke, myocardial infarction or revascularization, cardiac pacemaker or implantable defibrillator, cerebral aneurysm clip, neural stimulator, any type of ear implant, ocular foreign body, any implanted device, pregnant or breast-feeding female subjects, claustrophobia, allergy against gadolinium compounds, serum creatinine ≥ 1.3mg/dl).

Imaging protocol and data acquisition

MR examinations were performed in supine position on a 3-Tesla Magnetom Skyra (Siemens Healthineers, Erlangen, Germany) using an 18-channel body surface coil in combination with the table-mounted spine matrix coil. The complete imaging protocol as well as technical specificities have been described in detail elsewhere.[23]

The imaging protocol included a T2*-corrected, multi-echo 3D-gradient-echo Dixon-based sequence (multi-echo Dixon), originally determined for liver fat quantification[24,25] but also suited for the measurement of skeletal muscle size and adipose content and.[18–21] This multi-echo Dixon method is based on a prototype VIBE sequence with the following parameters: time to repetition (TR) 8.90ms, time to echo (TEs) opposed-phase 1.23ms, 3.69ms and 6.15ms, TEs in-phase 2.46ms, 4.92ms and 7.38ms, flip angle 4°, readout echo bandwidth 1080Hz/pixel, matrix 256x256, partition thickness 4mm. Data were acquired during a single breath-hold of 15s. The post-processing algorithm using the Software LiverLab (Version VD13, Siemens Healthineers, Cary, USA) automatically calculated water- and fat-only images as DICOM-files from the original data of the multi-echo acquisitions. The fat signal fraction maps are based on the signal ratio of fat to the summed signal of

water and fat (proton-density fat-fraction) and corrected for confounding effects of T1- and T2*-decay, quantitatively coding the mean proton-density fat-fraction (PDFF) in degrees of grey values of each voxel (1 grey value=0.1% adipose content).[24,25] Furthermore, for the correct location of L3 vertebra on axial slices, coronal two-point Dixon gradient-echo (GRE) sequences (TR 4.06ms, TE 1.26ms and 2.49ms, flip angle 9°, partition thickness 1.7mm, isotropic in-plane resolution 1.7mm) were used.

MR image analysis

    To determine the inter-observer reproducibility, two blinded observers (observer A and observer B) independently performed image analysis of 50 randomly selected KORA-data sets. For the assessment of intra-observer reproducibility, observer A repeated the analysis of all 50 data sets in a random order at least four weeks after the first reading in order to reduce recall bias. All analyses were performed in a blinded fashion, unaware of any information or clinical covariates of the subjects. Standard display settings were chosen to maximize the contrast between skeletal muscle and surrounding tissue. If necessary, the observers made manual adjustments for the best image contrast. Both readers had full access to scroll through all image data sets.

    Observer A and observer B both measured skeletal muscle adipose content as mean PDFF in percent (%) and skeletal muscle mass as muscle cross-sectional area (CSA) in square millimeters (mm^2) of the right (R) and left (L) psoas major muscle (MPM), quadratus lumborum muscle (MQL), autochthonous back muscles (ABM, containing the erector spinae muscles and the spinotransverse muscles) and rectus abdominis muscle (MRA) using dedicated, commercially available Software (Osirix V8.5.1, Pixmeo SARL, Bernex, Switzerland and MITK V2015.5.2, German Cancer Research Center, Heidelberg, Germany, respectively) on an offline workstation (Figure 1 and 2). The reliability of these methods has been validated previously.[18,19,26,27]

    Image analysis was performed on one axial slice at the level of the lower endplate of L3 vertebra, since recent studies demonstrated that skeletal muscle cross-sectional area at level L3 is a reliable method for the determination of sarcopenia[27] and quantification of skeletal muscle adipose content at level L4 and L3 vertebra are good surrogates for the entire lumbar spine.[28] The correct axial slice position was verified by identifying L4 vertebra by the iliac crest tangent sign on

coronal images using cross-reference (Figure 3).[29] If there were significant image artifacts limited to level L3 vertebra, the next possible, cranial slice without artifacts was selected for image analysis.

Each muscle compartment was analyzed by a standardized and manual segmentation method on the selected axial slice. ROIs determining CSA were drawn exactly on the muscle boundaries, comprising the whole muscle area, whereas ROIs quantifying PDFF were drawn a few voxels smaller concentrically in order to avoid partial volume effects of surrounding adipose tissue. Dedicated and standardized, anatomical landmarks were used to define the boundaries of the analyzed muscle compartments (Table 1 and Figure 4).

Covariates

A comprehensive health assessment prospectively collecting demographics and other cardiovascular risk factors was performed for all subjects. In this analysis, we included gender, age in years, body weight measured in kilograms (kg) and body height measured in centimeters (cm). The body mass index (BMI) was calculated as weight in kg divided by height in square meters (m^2). Waist circumference was measured at the smallest abdominal girth or, in obese subjects, in the midpoint of the lowest rib and the upper margin of the iliac crest and hip circumference was determined at the most protruding part of the hips to the nearest 1mm. In addition, visceral und subcutaneous adipose tissue (VAT and SCAT) were segmented and quantified in cm^2 by an automated algorithm based on fuzzy-clustering on one axial slice at the level of the umbilicus[30,31].

Statistical analysis

Descriptive characteristics were expressed as mean±standard deviation (SD) for continuous variables and percentages for categorical variables. Inter- and intra-observer reproducibility was assessed using scatter plots with Pearson correlations coefficients and intra-class correlation coefficients (ICC) from two-way random-effects ANOVA[32] as well as Bland-Altman plots with mean absolute differences±SD and 95%-limits of agreement. In addition, relative differences between the two observers were calculated and presented as mean±SD. An ICC-value close to 1 indicates excellent agreement between the two observers or observations. Analyses were repeated in subgroups (median divided) of age, gender, BMI, body height and

CSA. Statistical analysis was performed using Stata (V14.1, Stata Corporation, College Station, USA).

RESULTS

Study population

A total of 50 randomly selected subjects from the entire study population (n=400) were included in this analysis (mean age 56.1±8.8years, 60.0% males, mean BMI 28.3±5.2, mean body height 172.0±9.3cm^2). No subject was excluded due to impaired image quality. Demographics of the study population are provided in Table 2. For the assessment of inter- and intra-observer reproducibility of PDFF and CSA, a total of 1'200 measurements each were obtained.

Inter-observer reproducibility

The inter-observer agreement of PDFF was excellent for all muscle compartments (ICC 0.94 to 1.0) (Table 3). Similarly, inter-observer reproducibility of CSA was excellent for all included muscles (ICC 0.93 to 0.97) (Table 4). PDFF- and CSA-measurements were both highly correlated between the two separate measurements by observer A and observer B (r=0.99, ICC 0.99 and r=0.99, ICC 0.98, respectively, Figure 5 and Figure 6) with only minor mean absolute differences (mean absolute differences PDFF: -0.2±0.5% and CSA: 31.0±44.7mm^2, respectively). The mean variability was likewise very small for PDFF and CSA (mean relative difference PDFF: -2.6±6.4% and CSA: 2.7±3.9%, respectively) (Table 3 and Table 4).

Intra-observer reproducibility

For all analyzed muscle compartments, intra-observer reproducibility was excellent regarding PDFF (ICC 0.96 to 1.0) and CSA (ICC 0.96 to 0.98) (Table 3 and Table 4). PDFF- and CSA-measurements were highly correlated between the first and second reading by the same observer A (r=1.00, ICC 1.00 each, Figure 7 and Figure 8). The mean absolute and relative intra-observer differences were extremely small for both PDFF and CSA (mean absolute differences PDFF: 0.0±0.4% and CSA: 5.5±25.3mm^2; mean relative differences PDFF: 0.4±3.8% and CSA: 0.5±2.3%; respectively) (Table 3 and Table 4).

Effects of age, gender, BMI, body height and skeletal muscle mass on reproducibility

All agreement of PDFF and CSA was independent of age (PDFF: ICC 0.98 to 0.99 and CSA: ICC 0.97 to 1.0), gender (PDFF: ICC 0.99 to 1.0 and CSA: ICC 0.96 to 0.99), BMI (PDFF: ICC 0.98 to 1.0 and CSA: ICC 0.97 to 1.0) and body height (PDFF: ICC 0.97 to 1.0 and CSA: ICC 0.97 to 0.99) (Table 5 and Table 6). The mean differences of PDFF and CSA were similar between younger subjects (< 55years), male gender, non-obese subjects (BMI < 28.0) or subjects with a smaller body height (< 171.0cm) (for all ICC > 0.96). Furthermore, reproducibility of PDFF was independent of CSA (ICC 0.93 to 0.99).

DISCUSSION

Given their high potential as physical and metabolic biomarkers of myosteatosis and sarcopenia, we studied the reproducibility of the assessment of skeletal muscle adipose content and mass by MRI in a sample from the general population. Our results indicate that both PDFF and CSA by MRI are highly reproducibly using a standardized, multi-echo Dixon-based, manual segmentation method. Also, the measurement variabilities are independent of potential confounders, such as age, gender, BMI and body height as well as of each other.

Due to the highly relevant functional aspects and clinical significance of skeletal muscle, there are different methods being used for imaging and analysis of skeletal muscle composition, including for instance computed tomography, dual-energy X-ray absorptiometry or histopathology.[33] However, disadvantages of these approaches are the necessity of ionizing radiation and their invasiveness. Recent studies demonstrated that large-volume image-based (for example multi-echo Dixon) and spectroscopic fat-signal fractions agree well, thus providing a fast and accurate method for the quantification of skeletal muscle fat spezies.[19] Hence, besides other possible MRI-approaches, chemical-shift MRI, as used in this study, has been considered as the contemporary standard for the evaluation of skeletal muscle composition, structure and size providing reliable measurements also for minor changes.[18–21] To our knowledge, this is the first study reporting the reliability of skeletal muscle parameters by MRI in a larger cohort setting using a standardized approach based on distinct anatomical landmarks of the lumbar spine.

In contrast, we extend earlier observations of the high reproducibility of PDFF-measurements in the supraspinatus muscle.[18] In this study, Agten et al. found that the quantification of adipose content in the supraspinatus muscle by multi-echo Dixon is a reliable method and comparable to MR-spectroscopy. Similar to our approach, their results indicate substantial to almost perfect inter- and intra-observer agreement of PDFF-measurements (ICC 0.76 to 0.89). Their approach was similarly based on chemical-shift MRI and sample ROI PDFF-quantification of the entire muscle cross-sectional area.

Furthermore, our results agree well with CT-based evaluations, as a recent study by Jones et al. demonstrated good inter-observer reproducibility of the psoas muscle cross-sectional area as a reliable marker for sarcopenia using native CT acquisitions.[27] The reported parameters of agreement indicated good inter-observer

reproducibility (r^2=0.97, 95%-CI 0.89 to 0.98, p=0.001), although the study population consisted of clinical patients undergoing elective resection of colorectal carcinoma. Our findings therefore confirm prior results that an imaging-based assessment of skeletal muscle composition is a reliable biomarker and extend these observations to MRI, which may be particularly suited for asymptomatic subjects.

Regarding skeletal muscle adipose content, the applied anatomical landmark-based approach takes into account that extramyocellular-intrafascial adipose tissue may exert special metabolic and structural functions and could potentially compromise the functional capacity of myocytes and muscle tissue.[34] Thus, extramyocellular-extramyofascial adipose tissue adjacent to muscle tissue has to be separated accurately from intrafascial adipose tissue and should therefore be excluded regarding skeletal muscle composition analysis. Since recent studies demonstrated the functional properties of skeletal muscle and skeletal muscle adipose tissue as an endocrine organ, further studies will have to discriminate the different properties of intra- and intermyocellular-intrafascial lipids and adipose tissue regarding different metabolic and musculoskeletal disorders.

As a consequence, both PDFF and CSA as distinct skeletal muscle parameters may serve as robust biomarkers for myosteatosis and sarcopenia and may therefore be implemented also in large, population-based cohort studies. Two current examples are the German National Cohort[35] and the imaging enhancement program of the UK Biobank.[36] As part of those and other ongoing studies, the value of these biomarkers, in a socioeconomic and potentially clinical context, will be determined. Furthermore, given the high prevalence of DM and sarcopenia, further research on potential correlations, comorbidities and complications of both diseases based on the standardized approach evaluated in this study will be provided.

Our study has some limitations. First, this study is limited to data on the inter- and intra-observer variability focusing on observer and observing differences of skeletal muscle parameters. The results were not compared to a gold standard, such as histopathology for skeletal muscle adipose content or dual-energy X-ray absorptiometry for skeletal muscle mass. However, former studies have demonstrated the accuracy and reliability of the methods used in this study.[19,27]

Second, our approach for the quantification of skeletal muscle adipose content and mass was based on a manual segmentation. This may limit the application

possibility particularly with regard to very large cohort settings. Therefore, more advanced post-processing techniques, for example automatic or semiautomatic segmentation tools and implementation within image analysis pipelines will be necessary.

Third, sample ROI-measurements on one single axial slice at level L3 vertebra, as performed in this study, may not reproduce a heterogeneous distribution of mass and steatosis within the entire muscle due to under-sampling. However, recent studies showed that level L4 and L3 vertebra represent very good surrogates for the entire lumbar spine.[27,28] A single level-based PDFF- and CSA-measurement may therefore represent a valid and cost-effective approach to the assessment of sarcopenia and myosteatosis.

Conclusions

Quantification of skeletal muscle parameters, such as skeletal muscle adipose content and mass, using a standardized, anatomical landmark-based, manual segmentation of multi-echo Dixon data sets provides excellent inter- and intra-observer reproducibility. Thus, these parameters may serve as robust and reliable biomarkers, particularly in large cohort studies, providing new insights into the role of skeletal muscle in different disease states and potentially enhance metabolic and musculoskeletal risk stratification in healthy, asymptomatic and symptomatic subjects.

REFERENCES

1. Iizuka K, Machida T, Hirafuji M. Skeletal Muscle Is an Endocrine Organ. J Pharmacol Sci. 2014;125:125–31.

2. Giudice J, Taylor JM. Muscle as a paracrine and endocrine organ. Curr Opin Pharmacol [Internet]. 2017;34:49–55. Available from: http://dx.doi.org/10.1016/j.coph.2017.05.005

3. Warburton DER, Nicol CW, Bredin SSD. Health benefits of physical activity: the evidence. C Can Med Assoc J [Internet]. 2006;174(6):801–9. Available from: http://www.ncbi.nlm.nih.gov/pubmed/16534088%255Cnhttp://www.pubmedcentral.nih.gov/articlerender.fcgi?artid=PMC1402378

4. Ding D, Lawson KD, Kolbe-Alexander TL, Finkelstein EA, Katzmarzyk PT, van Mechelen W, et al. The economic burden of physical inactivity: a global analysis of major non-communicable diseases. Lancet [Internet]. 2016;388(10051):1311–24. Available from: http://dx.doi.org/10.1016/S0140-6736(16)30383-X

5. Machann J, Häring H, Shick F, Stumvoll M. Intramyocellular lipids and insulin resistance. Diabetes, Obes Metab. 2004;6(4):239–48.

6. Jacob S, Machann J, Rett K, Brechtel K, Volk A, Renn W, et al. Association of Increased Intramyocellular Lipid Content With Insulin Resistance in Lean Nondiabetic Offspring of Type 2 Diabetic Subjects. Diabetes. 1999;48(21):1113–9.

7. Boettcher M, Machann J, Stefan N, Thamer C, Häring H-U, Claussen CD, et al. Intermuscular adipose tissue (IMAT): Association with other adipose tissue compartments and insulin sensitivity. J Magn Reson Imaging. 2009;29(6):1340–5.

8. Volpato S, Bianchi L, Lauretani F, Lauretani F, Bandinelli S, Guralnik JM, et al. Role of muscle mass and muscle quality in the association between diabetes and gait speed. Diabetes Care. 2012;35(8):1672–9.

9. Park SW, Goodpaster BH, Lee JS, Kuller LH, Boudreau R, De Rekeneire N, et al. Excessive loss of skeletal muscle mass in older adults with type 2 diabetes. Diabetes Care [Internet]. 2009;32(11):1993–7. Available from: http://care.diabetesjournals.org/content/32/11/1993.short

10. International Diabetes Federation. Diabetes Atlas. IDF Diabetes Atlas 7th Edition 2015. 2015.

11. Haehling S von, Morley JE, Anker SD. An overview of sarcopenia : facts and numbers on prevalence and clinical impact. J Cachexia Sarcopenia Muscle. 2010;1:129–33.

12.   Wang T, Feng X, Zhou J, Gong H, Xia S, Wei Q, et al. Type 2 diabetes mellitus is associated with increased risks of sarcopenia and pre-sarcopenia in Chinese elderly. Nature. 2016;6(38937):1–7.

13.   Bouchi R, Fukuda T, Takeuchi T, Nakano Y, Murakami M, Minami I, et al. Association of sarcopenia with both latent autoimmune diabetes in adults and type 2 diabetes: a cross-sectional study. J Diabetes Complications [Internet]. 2017;31(6):992–6. Available from: http://dx.doi.org/10.1016/j.jdiacomp.2017.02.021

14.   Volpato S, Blaum C, Resnick H, Ferrucci L, Fried LP, Guralnik JM. Comorbidities and Impairments Explaining the Association Between Diabetes and Lower Extremity Disability - The Women' s Health and Aging Study. Diabetes Care. 2001;25(4):678–83.

15.   Brøns C, Grunnet LG. Skeletal muscle lipotoxicity in insulin resistance and type 2 diabetes: a causal mechanism or an innocent bystander? Eur J Endocrinol [Internet]. 2017;176(2):R67–78. Available from: http://www.eje-online.org/lookup/doi/10.1530/EJE-16-0488

16.   Miljkovic I, Kuipers A, Cvejkus R, Bunker C, Patrick A, Gordon C, et al. Myosteatosis increases with aging and is associated with incident diabetes in African ancestry men. Obes (Silver Spring). 2016;16(3):338–48.

17.   Phillips A, Strobl R, Vogt, Ladwig K-H, Thorand B, Grill E. Sarcopenia is associated with disability status - results from the KORA-Age study. Osteoporos Int. 2017;28:2069–79.

18.   Agten CA, Rosskopf AB, Gerber C, Pfirrmann CWA. Quantification of early fatty infiltration of the rotator cuff muscles: comparison of multi-echo Dixon with single-voxel MR spectroscopy. Eur Radiol [Internet]. 2016;26(10):3719–27. Available from: http://dx.doi.org/10.1007/s00330-015-4144-y

19.   Fischer MA, Nanz D, Shimakawa A, Schirmer T, Guggenberger R, Chhabra A, et al. Quantification of Muscle Fat in Patients with Low Back Pain: Comparison of Multi-Echo MR Imaging with Single-Voxel MR Spectroscopy. Radiology. 2013;266(2):555–63.

20.   Elliott JM, Courtney DM, Rademaker A, Pinto D, Sterling MM, Parrish TB. The Rapid and Progressive Degeneration of the Cervical Multifidus in Whiplash: A MRI study of Fatty Infiltration. Spine (Phila Pa 1976). 2015;33(4):395–401.

21.   Reeder SB, Hu HH, Sirlin CB. Proton Density Fat-Fraction: A Standardized MR-Based Biomarker of Tissue Fat Concentration. J Magn Reson Imaging. 2016;36(5):1011–4.

22.   Holle R, Happich M, Löwel H, Wichmann H. KORA - A Research Platform for Population Based Health Research. Das Gesundheitswes [Internet]. 2005;67(1):19–25. Available from: http://www.thieme-connect.de/DOI/DOI?10.1055/s-2005-858235

23.   Bamberg F, Hetterich H, Rospleszcz S, Lorbeer R, Auweter SD, Schlett CL, et al. Subclinical disease burden as assessed by whole-body MRI in subjects with prediabetes, subjects with diabetes, and normal control subjects from the general population: The KORA-MRI study. Diabetes. 2017;66(1):158–69.

24.   Zhong X, Nickel MD, Kannengiesser SAR, Dale BM, Kiefer B, Bashir MR. Liver fat quantification using a multi-step adaptive fitting approach with multi-echo GRE imaging. Magn Reson Med. 2014;72(5):1353–65.

25.   Bashir MR, Zhong X, Nickel MD, Fananapazir G, Kannengiesser SAR, Kiefer B, et al. Quantification of hepatic steatosis with a multistep adaptive fitting MRI approach: Prospective validation against MR spectroscopy. Am J Roentgenol. 2015;204(2):297–306.

26.   Crawford RJ, Cornwall J, Abbott R, Elliott JM. Manually defining regions of interest when quantifying paravertebral muscles fatty infiltration from axial magnetic resonance imaging: a proposed method for the lumbar spine with anatomical cross-reference. BMC Musculoskelet Disord [Internet]. 2017;18(1):25. Available from: http://bmcmusculoskeletdisord.biomedcentral.com/articles/10.1186/s12891-016-1378-z

27.   Jones KI, Doleman B, Scott S, Lund JN, Williams JP. Simple psoas cross-sectional area measurement is a quick and easy method to assess sarcopenia and predicts major surgical complications. Color Dis. 2014;17:20–6.

28.   Crawford RJ, Filli L, Elliott JM, Nanz D, Fischer MA, Marcon M, et al. Age- and Level-Dependence of Fatty Infiltration in Lumbar Paravertebral Muscles of Healthy Volunteers. Spine (Phila Pa 1976). 2016;37:742–8.

29.   Farshad-Amacker NA, Aichmair A, Herzog RJ, Farshad M. Merits of different anatomical landmarks for correct numbering of the lumbar vertebrae in lumbosacral transitional anomalies. Eur Spine J. 2015;24:600–8.

30.   Würslin C, Machann J, Rempp H, Claussen C, Yang B, Schick F. Topography mapping of whole body adipose tissue using a fully automated and standardized procedure. J Magn Reson Imaging. 2010;31(2):430–9.
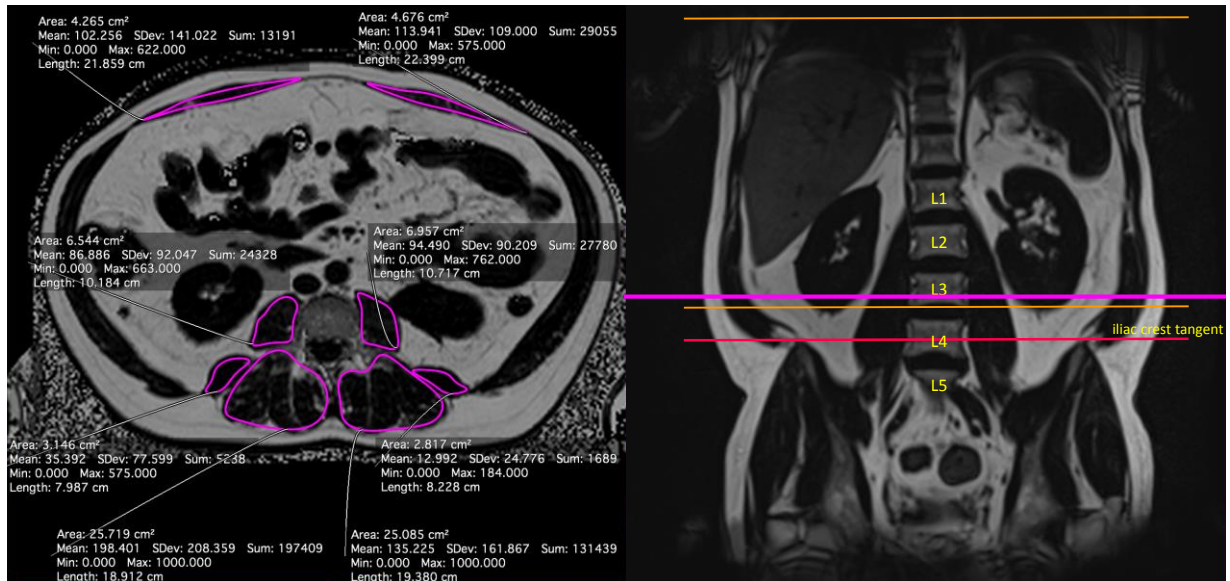
31.   Schwenzer NF, Machann J, Schraml C, Springer F, Ludescher B, Stefan N, et al. Quantitative Analysis of Adipose Tissue in Single Transverse Slices for Estimation of Volumes of Relevant Fat Tissue Compartments: A Study in a Large Cohort of Subjects at Risk for Type 2 Diabetes by MRI with Comparison to Anthropometric Data. Invest Radiol [Internet]. 2010;45(12):788–94. Available from: http://www.ncbi.nlm.nih.gov/pubmed/20829704

32.   Shrout PE, Fleiss JL. Intraclass Correlations: Uses in Assessing Rater Reliability. Psychol Bull. 1979;86(2):420–8.

33.   Lemos T, Gallagher D. Current body composition measurement techniques. Curr Opin Endocrinol Diabetes Obes [Internet]. 2017;24(5):1. Available from: http://insights.ovid.com/crossref?an=01266029-900000000-99433

34.   Shahidi B, Parra CL, Berry DB, Hubbard JC, Gombatto S, Zlomislic V, et al. Contribution of Lumbar Spine Pathology and Age to Paraspinal Muscle Size and Fatty Infiltration. Spine (Phila Pa 1976). 2017;42(8):616–23.

35.   Schlett CL, Hendel T, Weckbach S, Reiser M, Kauczor HU, Nikolaou K, et al. Population-Based Imaging and Radiomics : Rationale and Perspective of the German National Cohort MRI Study. Fortschr Röntgenstr. 2016;188:652–61.

36.   Sudlow C, Gallacher J, Allen N, Beral V, Burton P, Danesh J, et al. UK Biobank: An Open Access Resource for Identifying the Causes of a Wide Range of Complex Diseases of Middle and Old Age. PLoS Med. 2015;12(3):1–10.
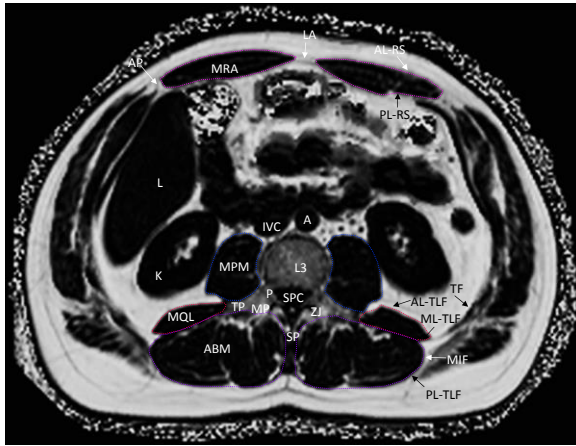
FIGURES
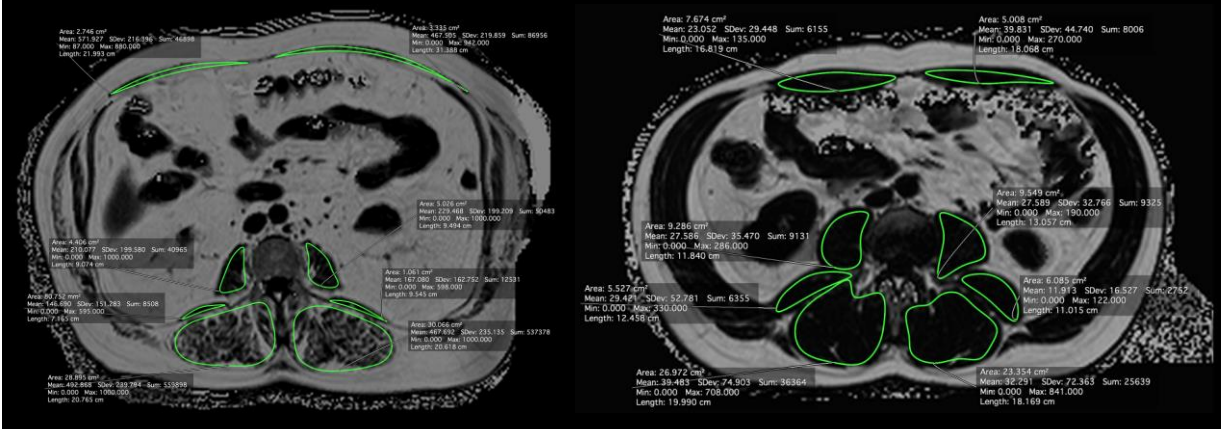
Figure 1 Skeletal muscle adipose content by PDFF.

Skeletal muscle adipose content as mean PDFF in one ROI at level L3 vertebra.

Figure 2 Skeletal muscle mass by CSA.

Skeletal muscle mass as CSA by an anatomical landmark-based, manual segmentation at level L3 vertebra.

Figure 3 Validation of the correct axial slice position at the level of the lower endplate of L3 vertebra.

Identification of level L3 vertebra by the iliac crest tangent sign, marking either L4 vertebra or L4/5 intervertebral disc.

**Figure 4** Standardized, anatomical landmarks defining muscle compartments.

MPM - psoas major muscle (blue ROIs), MQL - quadratus lumborum muscle (red ROIs), ABM - autochthonous back muscles (purple ROIs), MRA - rectus abdominis muscle (pink ROIs), L3 - lumbar vertebral body 3, TP - transverse process, MP - mammillary process, P - pedicle of the vertebral arch, ZJ - zygapophyseal joint, SP - spinous process, SPC - spinal canal, AL-TLF - anterior lamina of the thoracolumbar fascia, ML-TLF - middle lamina of the thoracolumbar fascia, PL-TLF - posterior lamina of thoracolumbar fascia, TF - transverse fascia, AP - aponeuroses of the transverse abdominal & the external and internal oblique muscles, AL-RS - anterior lamina of the rectus sheath, PL-RS - posterior lamina of the rectus sheath, LA - linea alba
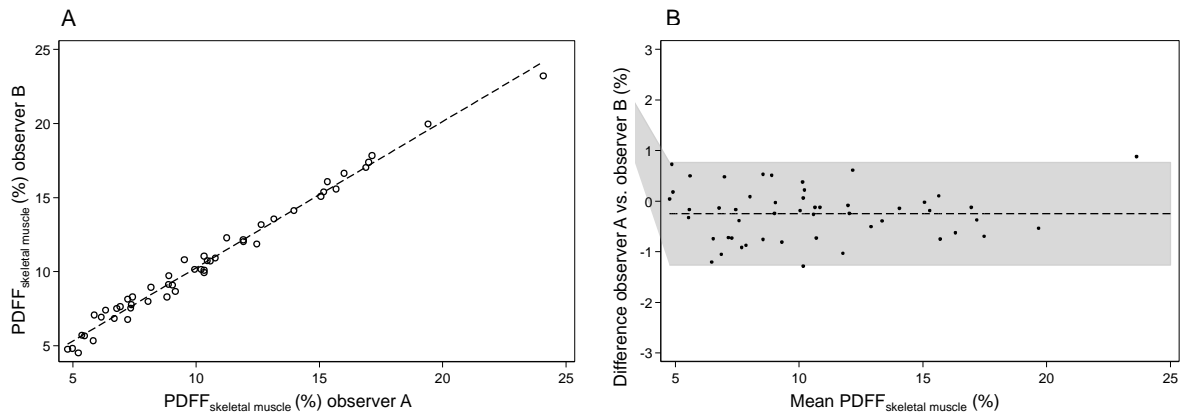
Figure 5: Inter-observer correlation of PDFF.

(A) Scatter plot of the PDFF$_{skeletal\ muscle}$ inter-observer correlation demonstrating the linear correlation between observer A and observer B (r = 0.99, ICC = 0.99).
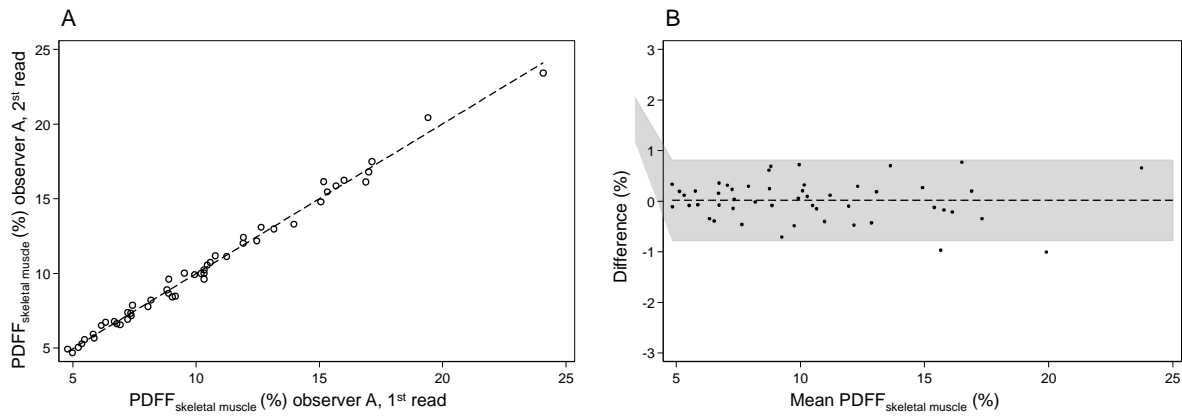
(B) Bland-Altman plot of the same data. Mean difference: -0.249 (CI -0.396 to -0.102), range 4.767 to 23.639, 95% limits of agreement (reference range for difference): -1.262 to 0.764.
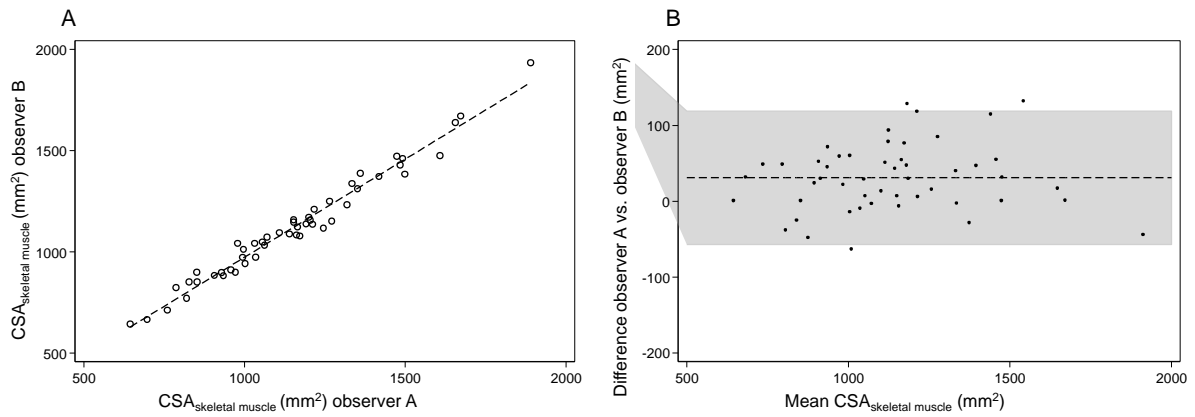
Figure 6: Inter-observer correlation of CSA.

(A) Scatter plot of the $CSA_{skeletal\ muscle}$ inter-observer correlation demonstrating the linear correlation between observer A and observer B (r = 0.99, ICC = 0.98).
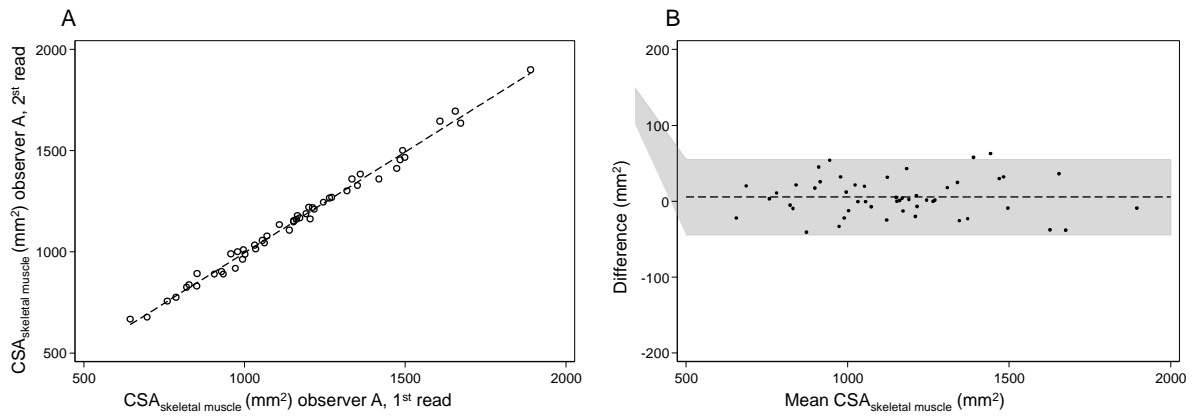
(B) Bland-Altman plot of the same data. Mean difference: 30.959 (CI 18.242 to 43.676), range 643.887 to 1912.458, 95% limits of agreement (reference range for difference): -56.743 to 118.661.

Figure 7: Intra-observer correlation of PDFF.

(A) Scatter plot of the PDFF$_{skeletal\ muscle}$ intra-observer correlation demonstrating the linear correlation between the 1st and 2nd observing by observer A (r = 1.00, ICC 1.00).

(B) Bland-Altman plot of the same data. Mean difference: 0.018 (CI -0.097 to 0.132), range 4.830 to 23.751, 95% limits of agreement (reference range for difference): -0.773 to 0.808.

Figure 8: Intra-observer correlation of CSA.

> **(A)** Scatter plot of the $CSA_{skeletal\ muscle}$ intra-observer correlation demonstrating the linear correlation between the 1st and 2nd observing by observer A (r = 1.00, ICC = 1.00).

> **(B)** Bland-Altman plot of the same data. Mean difference: 5.490 (CI -1.702 to -12.682), range 655.546 to 1895.119, 95% limits of agreement (reference range for difference): -44.110 to 55.089.

TABLES

Psoas major muscle (MPM)	Quadratus lumborum muscle (MQL)
- anteriolateral: transverse fascia - medial: L3 vertebral body - medioposterior: pedicle of the vertebral arch & transverse process - posteriolateral: anterior & middle lamina of the thoracolumbar fascia[1]	- anterior: transverse fascia - anteriomedial: anterior lamina of the thoracolumbar fascia[1] - posterior: transverse process - lateral: anterior & middle lamina of the thoracolumbar fascia[1]
Autochthonous back muscles (ABM)	**Rectus abdominis muscle (MRA)**
- anterior: transverse process & middle lamina of the thoracolumbar fascia[2] - medial: mammillary process, zygapophyseal joint & spinous process[3] - lateral: rounded fascial boundary of M. iliocostalis - posterior: posterior lamina of the thoracolumbar fascia[4]	- anterior: anterior lamina of the rectus sheath - medial: linea alba - posterior: posterior lamina of the rectus sheath & transverse fascia - lateral: aponeuroses of the transverse abdominal & the external and internal oblique muscles[5]

Table 1 Anatomical landmarks defining the muscle boundaries.

[1] Separating MQL from MPM: Adipose tissue between the muscle fascia was excluded from the ROI defining MPM and MQL due to its extramyofascial location. [2] Separating ABM from MQL: Adipose tissue between the muscle fascia was excluded from the ROI defining ABM due to its extramyofascial location. [3] Adipose tissue approximating the spinous or mammillary process was included within the ROI defining ABM, due to its intramyofascial location. [4] If a fat-filled triangular exists within the thoracolumbar fascia posteriorly between the longissimus and the iliocostalis muscle, it was included within the ROI of ABM due to its intramyofascial location. [5] Adipose tissue between the aponeuroses of the transverse abdominal & the external and internal oblique muscles was excluded from the ROI defining MRA due to its extramyofascial location.

Characteristics	All subjects	Female	Male
N	50	20	30
Age (years)	56.1±8.8	56.7±9.5	55.8±8.4
BMI (kg/m^2)	28.3±5.2	27.8±6.4	28.5±4.2
Body weight (kg)	83.8±17.3	75.8±18	89.2±14.8
Body height (cm)	172.0±9.3	165.1±6.6	176.6±7.8
Waist circumference (cm)	97.9±14.5	90.1±15.3	103.1±11.5
Hip circumference (cm)	106.7±10	107.4±12.8	106.2±7.7
VAT (cm^2)	156.1±95	100.8±64.9	193.7±94.6
SCAT (cm^2)	290.4±123.1	318.5±154.4	271.4±94.8

Table 2 Demographics of the study population. Data is presented as mean±standard deviation.

	Inter-observer variability PDFF			Intra-observer variability PDFF		
	ICC (95%-CI)	**Difference (mean±SD)**		**ICC (95%-CI)**	**Difference (mean±SD)**	
		Absolute (%)	Relative (%)		Absolute (%)	Relative (%)
Psoas major muscle (right)	0.94 (0.89;0.97)	-0.3±0.9	-3.7±13.6	0.96 (0.93;0.98)	0.1±0.8	1.4±12.0
Psoas major muscle (left)	0.98 (0.97;0.99)	-0.2±0.6	-2.1±9.3	0.98 (0.97;0.99)	-0.1±0.5	0.2±9.3
Quadratus lumborum muscle (right)	0.97 (0.96;0.99)	0.1±0.7	2.6±16.7	0.98 (0.96;0.99)	0.1±0.7	1.8±14.7
Quadratus lumborum muscle (left)	0.94 (0.9;0.97)	-0.1±0.8	0.4±17.6	0.98 (0.96;0.99)	0.1±0.5	1.4±10.7
Autochthonous back muscles (right)	0.98 (0.96;0.99)	-0.6±1.5	-3.4±10.9	0.99 (0.98;0.99)	-0.2±1.2	-1.1±7.2
Autochthonous back muscles (left)	0.99 (0.98;0.99)	-0.3±1.3	-2.4±8.7	0.99 (0.99;1.0)	0.3±1.0	1.9±7.1
Rectus abdominis muscle (right)	1.0 (0.99;1.0)	-0.4±1.4	-5.9±17.3	1.0 (0.99;1.0)	0.1±1.5	-1.3±10.8
Rectus abdominis muscle (left)	0.99 (0.98;0.99)	-0.2±1.4	-2.8±14.4	0.99 (0.97;0.99)	-0.2±1.5	-0.1±13.2
Mean skeletal muscle (bilaterally)	0.99 (0.98;1.0)	-0.2±0.5	-2.6±6.4	1.0 (0.99;1.0)	0.0±0.4	0.4±3.8

Table 3 Inter- and intra-observer reproducibility of PDFF. ICC: intra-class correlation coefficient, CI: confidence interval.

	Inter-observer variability CSA			Intra-observer variability CSA		
	ICC (95%-CI)	**Difference (mean±SD)**		**ICC (95%-CI)**	**Difference (mean±SD)**	
		Absolute (mm^2)	Relative (%)		Absolute (mm^2)	Relative (%)
Psoas major muscle (right)	0.93 (0.88;0.96)	19.5±105.0	2.5±8.6	0.98 (0.97;0.99)	2.4±47.8	-0.1±6.0
Psoas major muscle (left)	0.97 (0.94;0.98)	7.0±66.8	0.6±8.1	0.97 (0.95;0.98)	10.5±60.9	0.6±7.0
Quadratus lumborum muscle (right)	0.95 (0.92;0.97)	13.0±59.2	2.6±18.5	0.97 (0.96;0.99)	4.2±44.9	1.0±10.7
Quadratus lumborum muscle (left)	0.96 (0.93;0.98)	2.5±49.4	1.7±14.0	0.97 (0.94;0.98)	-15.7±40.8	-4.6±11.1
Autochthonous back muscles (right)	0.97 (0.94;0.99)	58.3±118	2.2±5.1	0.98 (0.97;0.99)	2.8±108.8	0.2±4.4
Autochthonous back muscles (left)	0.97 (0.94;0.98)	33.3±132.1	1.2±5.4	0.98 (0.97;0.99)	22±95.4	1.0±3.5
Rectus abdominis muscle (right)	0.93 (0.57;0.98)	72.2±70.0	10.7±11.6	0.96 (0.94;0.98)	15.9±74.8	3.2±11.7
Rectus abdominis muscle (left)	0.95 (0.89;0.97)	41.9±93.0	5.2±12.3	0.98 (0.97;0.99)	1.8±59.1	0.5±9.3
Mean skeletal muscle (bilaterally)	0.98 (0.93;0.99)	31±44.7	2.7±3.9	1.0 (0.99;1.0)	5.5±25.3	0.5±2.3

Table 4 Inter- and intra-observer reproducibility of CSA. ICC: intra-class correlation coefficient, CI: confidence interval.

	Inter-observer variability PDFF			Intra-observer variability PDFF		
	ICC (95%-CI)	**Difference (mean±SD)**		**ICC (95%-CI)**	**Difference (mean±SD)**	
		Absolute (%)	Relative (%)		Absolute (%)	Relative (%)
Age < 55years	0.98 (0.92;0.99)	-0.3±0.5	-3.5±6.9	0.99 (0.98;1.0)	0.1±0.3	1.4±3.5
Age ≥ 55years	0.99 (0.98;1)	-0.2±0.5	-1.8±5.9	0.99 (0.99;1.0)	0±0.5	-0.6±3.9
Gender: male	0.99 (0.98;1.0)	-0.2±0.5	-1.6±6.6	0.99 (0.99;1.0)	0±0.4	0.4±4
Gender: female	0.99 (0.97;1)	-0.3±0.5	-4.1±5.9	1.0 (0.99;1.0)	0±0.4	0.2±3.7
BMI < 28.0	0.98 (0.92;0.99)	-0.3±0.5	-3.9±7.1	0.99 (0.98;1.0)	0±0.3	0±4.1
BMI ≥ 28.0	0.99 (0.99;1.0)	-0.2±0.5	-1.5±5.6	1.0 (0.99;1.0)	0±0.5	0.7±3.7
Height < 171.0cm	1.0 (0.99;1.0)	-0.2±0.4	-2.4±5.1	1.0 (0.99;1.0)	0±0.5	-0.1±3.5
Height ≥ 171.0cm	0.97 (0.92;0.99)	-0.3±0.6	-2.7±7.5	0.99 (0.98;1.0)	0±0.4	0.8±4.2
CSA_{MPMR} < 910.8925mm^2	0.95 (0.88;0.98)	-0.3±0.9	-4.5±14.3	0.95 (0.89;0.98)	0.1±0.9	1.1±13.4
CSA_{MPMR} ≥ 910.8925mm^2	0.93 (0.84;0.97)	-0.2±0.9	-2.8±13	0.97 (0.93;0.99)	0.1±0.6	1.6±10.6
CSA_{ABMR} < 2465.335mm^2	0.96 (0.89;0.99)	-1.0±1.7	-6.3±10.7	0.98 (0.96;0.99)	-0.3±1.4	-2.1±7.9
CSA_{ABMR} ≥ 2465.335mm^2	0.99 (0.97;0.99)	-0.3±1.2	-0.5±10.5	0.99 (0.98;1.0)	-0.2±0.9	-0.1±6.5

Table 5 Effects of age, gender, BMI, body height and muscle mass on the reproducibility of PDFF. ICC: intra-class correlation coefficient, CI: confidence interval.

	Inter-observer variability CSA			Intra-observer variability CSA		
	ICC (95%-CI)	**Difference (mean±SD)**		**ICC (95%-CI)**	**Difference (mean±SD)**	
		Absolute (mm^2)	Relative (%)		Absolute (mm^2)	Relative (%)
Age < 55years	0.99 (0.94;1)	28.1±39.6	2.6±3.2	1.0 (0.99;1.0)	0.9±27.3	0.1±2.2
Age ≥ 55years	0.97 (0.88;0.99)	33.4±49.4	2.9±4.5	0.99 (0.99;1.0)	9.4±23.2	0.8±2.3
Gender: male	0.97 (0.87;0.99)	35.6±47.5	2.8±3.7	0.99 (0.99;1.0)	5.2±26.1	0.4±1.9
Gender: female	0.96 (0.86;0.98)	24±40.4	2.5±4.3	0.99 (0.97;1.0)	5.9±24.7	0.6±2.7
BMI < 28.0	0.98 (0.94;0.99)	22.5±33.9	2.1±3.3	1.0 (0.99;1.0)	4.9±21.1	0.4±2.1
BMI ≥ 28.0	0.97 (0.89;0.99)	38.1±51.8	3.3±4.4	0.99 (0.99;1.0)	6.0±28.8	0.6±2.4
Height < 171.0cm	0.98 (0.93;0.99)	23.6±38.6	2.2±4.0	0.99 (0.98;1.0)	4.8±26.4	0.4±2.7
Height ≥ 171.0cm	0.97 (0.86;0.99)	37.8±49.5	3.2±3.9	0.99 (0.98;1.0)	6.1±24.8	0.6±1.8

Table 6 Effects of age, gender, BMI and body height on the reproducibility of CSA. ICC: intra-class correlation coefficient, CI: confidence interval.